ACS Medicinal Chemistry Letters

Letter

pubs.acs.org/acsmedchemlett

2-Hydroxypyridine-*N*-oxide-Embedded Aurones as Potent Human Tyrosinase Inhibitors

Romain Haudecoeur,*[,†,§] Marcello Carotti,[‡,§] Aurélie Gouron,[∥,§] Marc Maresca,[⊥] Elina Buitrago,[†,∥] Renaud Hardré,[⊥] Elisabetta Bergantino,[‡] Hélène Jamet,[∥] Catherine Belle,[∥] Marius Réglier,[⊥] Luigi Bubacco,[‡] and Ahcène Boumendjel[†]

[†]Univ. Grenoble-Alpes/CNRS, DPM UMR 5063, CS 40700, 38058 Grenoble, France

[‡]Department of Biology, University of Padova, Via Ugo Bassi 58b, Padova 35121, Italy

[∥]Univ. Grenoble-Alpes/CNRS, DCM UMR 5250, CS 40700, 38058 Grenoble, France

[⊥]Aix Marseille Univ, CNRS, Centrale Marseille, iSm2, Marseille, France

Supporting Information

ABSTRACT: With the aim to develop effective and selective human tyrosinase inhibitors, we investigated aurone derivatives whose B-ring was replaced by a non-oxidizable 2-hydroxypyridine-*N*-oxide (HOPNO) moiety. These aurones were synthesized and evaluated as inhibitors of purified human tyrosinase. Excellent inhibition activity was revealed and rationalized by theoretical calculations. The aurone backbone was especially found to play a crucial role, as the HOPNO moiety alone provided very modest activity on human tyrosinase. Furthermore, the *in vitro* activity was confirmed by measuring the melanogenesis suppression ability of the compounds in melanoma cell lysates and whole cells. Our study reveals that HOPNO-embedded 6-hydroxyaurone is to date the most effective inhibitor of isolated human tyrosinase. Owing to its low toxicity and its high inhibition activity, it could represent a milestone on the path toward new valuable agents in dermocosmetics, as well as in medical fields where it was recently suggested that tyrosinase could play key roles.

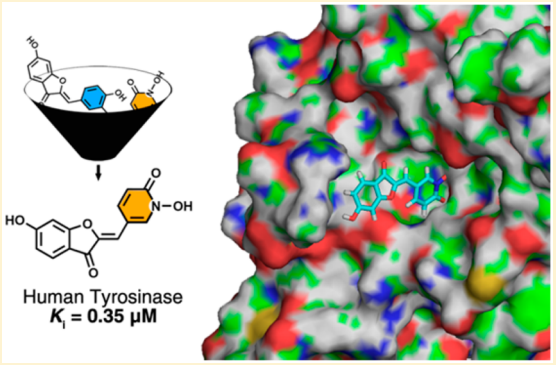

KEYWORDS: *Human tyrosinase, aurones, human melanoma, transition state analogues, QM/MM calculations*

Tyrosinases (Ty, EC 1.14.18.1) are type-3 copper-containing metalloenzymes spread across a wide range of organisms, especially mammals, fungi, bacteria, and plants.[1] These include a binuclear active site, composed by two close copper centers ($d_{Cu-Cu} \approx 2.9$ to 4.9 Å) bridged by an aquo(hydroxo) ligand in a met state, coordinated by six histidine residues. Ty catalyzes the oxidation of phenols and catechols into catechols and *ortho*-quinones, respectively (Scheme 1).[2] In mammals the transformations of Ty natural substrates, L-tyrosine and L-DOPA, into reactive quinones are the first steps of melanogenesis.[3] The resulting melanin pigments play a protecting role against UV radiation and free radicals. Despite similar dicopper active sites (see Supporting Information) and a common function, i.e., phenol/catechol oxidation, significant differences were pointed out at cellular and structural levels among the Tys from distinct sources, especially plant (TyP), mushroom (TyM), bacterial (TyB), and human (TyH).[4] Indeed, while TyM and TyB are generally soluble oligomeric enzymes present in the cytosol, TyH exists as a highly glycosylated monomeric melanosomal transmembrane protein.[5,6] Similarly, strong divergences are observed upon sequence comparison, a discrepancy that has been substantiated at a structural level in the past decade by the resolution of crystallographic structures of two TyB (from *Bacillus megaterium*, TyB1[7] and *Streptomyces castaneoglobisporus*, TyB2),[8] three TyM (from *Agaricus bisporus*, TyM1[9,10] and TyM2,[11,12] and *Aspergillus oryzae*, TyM3),[13] and very recently one TyP (from *Juglans regia*)[14] and one polyphenol oxidase exhibiting tyrosinase activity toward certain substrates (from *Coreopsis grandiflora*).[15,16] More precisely, the overall identity is low (10−30%) between TyMs, TyBs, and TyH. Around the active site (58% identity within 6 Å from the metal center in TyM1 and TyB2), the environments are similar (see Supporting Information), despite some key features not shared among all Tys (e.g., a conserved Cu_A histidine ligand cross-linked to a cysteine residue in TyMs and TyP, a post-translational modification absent in TyBs and TyH).[17] While preliminary crystallographic studies on TyH have been reported very recently, no structures are available to date at atomic resolution.[18] However, a robust homology model built using structural data from TyB2 and *Ipomea batatas* catechol oxidase has recently been published.[19]

Received: September 22, 2016
Accepted: November 17, 2016
Published: November 17, 2016

DOI: 10.1021/acsmedchemlett.6b00369
ACS Med. Chem. Lett. 2017, 8, 55−60

Scheme 1. Inhibition and Catalysis Pathways: Putative Interactions between HOPNO Derivatives and the Met Form of Ty

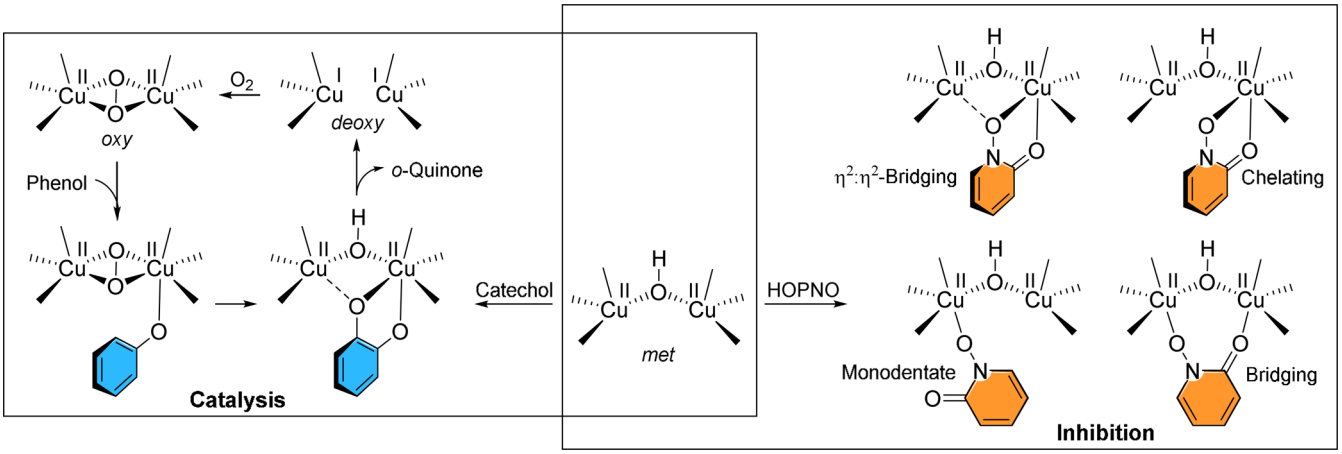

In humans, melanin-related disorders are known to cause cutaneous hyperpigmentation,[20] skin lesions,[21] or melanoma resistance to conventional therapies.[22] As Ty inhibition is a well-established strategy for controlling melanin production *in vivo*, as demonstrated again recently,[23] the development of TyH inhibitors raises considerable interest in dermocosmetics[24] and cancer therapies[25] fields. While the low homologies between the different forms of Ty exclude any extrapolation of inhibition studies performed on TyM to TyH, an abundant literature is dedicated to TyM inhibitors for human applications.[26] As a result, only a handful of them are actually in use as depigmentation agents, such as hydroquinone, arbutin, or kojic acid (KA).[27] Unfortunately, currently used inhibitors lack the affinity and selectivity required for TyH-targeting applications and harmful toxicity has often been reported.[4,28] Therefore, there is an urgent need for novel selective TyH inhibitors that match efficacy and safety standards required for the development of products aimed to human use.

Over recent years, we reported that aurones (2-benzylidene-benzofuran-3(2*H*)-ones), naturally occurring flavonoids,[29,30] act as inhibitors of melanin biosynthesis in human melanocytes,[31] as effectors of TyM,[32,33] and as molecular probes for the investigation of the binding-site structural homology between TyM and TyB.[17] In one of these previous studies,[32] we suggested that these compounds bind to the Ty active site with their B-ring, whose substituents determined the behavior of diverse aurones toward both enzymes (i.e., inhibitor, activator, or substrate). Conversely, the A-ring hydroxylation pattern of aurones affected the activity range and selectivity for either TyM1 or TyB3 (TyB from *Streptomyces antibioticus*, which belongs to the same *Streptomyces* genus and shares 82% identity with TyB2), sometimes considerably (aurones **V** in Figure 1). In parallel, we discovered and investigated the transition-state analogue HOPNO, a catechol-mimicking, non-oxidizable moiety (Scheme 1), as a potent inhibitor of TyM1 (K_{ic} = 1.8 μM).[34] Embedding this small moiety in an aurone backbone generated "hybrid" aurone **1a**, which showed a TyM1 inhibition activity in the same range as HOPNO (Figure 1).[32]

We report herein the synthesis of three hybrid aurones, whose A-ring substitution patterns were selected reminiscently of our previous results on human melanocytes,[31] along with their biological evaluation through *in vitro* assays using (1) purified recombinant TyH (from *Homo sapiens*) and (2) human MNT-1 melanoma cells. The interactions of the most active hybrid aurone with TyH were then rationalized by combining

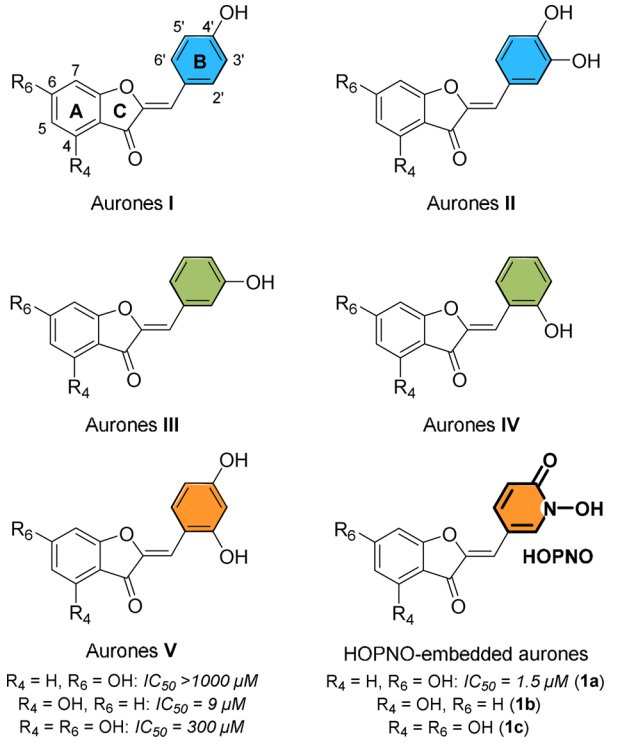

Figure 1. General structures of aurones previously identified as effectors of TyM1 and TyB3. These compounds were substrates (B-ring in blue), activators (B-ring in green), or inhibitors (B-ring in orange) of TyM1. For inhibitors, corresponding IC_{50} values against TyM1 are indicated.[17,32]

QM/MM dynamics and noncovalent interaction (NCI) analysis, using the recent homology model of TyH mentioned above.[19] Comparisons were made with the interactions of the HOPNO moiety alone on TyH.

As a whole, our recent studies highlighted a remarkable versatility of aurones as Ty-interacting agents, allowing us to gather valuable information on the relation between their substitution pattern and their activities.[17,31,32] The B-ring of aurones, as it interacts directly with the active site, completely determined their general behavior toward TyM1 and TyB3. Indeed, aurones **I** and **II** act as alternative substrates, aurones **III** and **IV** as activators (for TyM1) or weak inhibitors (for TyB3), and aurones **V** as mixed inhibitors (Figure 1). We also

DOI: 10.1021/acsmedchemlett.6b00369
ACS Med. Chem. Lett. 2017, 8, 55−60

Table 1. Protonation Constants, Inhibition Constants (K_i) on Purified TyH, IC_{50} on Human MNT-1 Melanoma Cells, and Cytotoxicity Values (IC_{50}) on MNT-1 Cells for Compounds 1a−c

	protonation constants			purified TyH	MNT-1 lysate	MNT-1 whole cells	MNT-1 cytotoxicity
compound	$pK_{4\text{-}OH}$	$pK_{6\text{-}OH}$	pK_{N-OH}	K_i (μM)	IC_{50} (μM)	IC_{50} (μM)	IC_{50} (μM)
1a		6.71 ± 0.05	5.40 ± 0.08	0.35 ± 0.04	16.6 ± 0.3	85.3 ± 0.6	>500
1b	7.57 ± 0.07		5.6 ± 0.1	1.02 ± 0.04	30 ± 2	120 ± 10	80 ± 20
1c	7.2 ± 0.1	8.3 ± 0.1	5.8 ± 0.1	1.2 ± 0.2	34 ± 3	119 ± 1	>500
HOPNO			6.07 ± 0.02[a]	128 ± 2	1300 ± 100	150 ± 20	>200
KA				350 ± 70[b]	2800 ± 800	15000 ± 2000	>80000

[a]See ref 35. [b]See ref 4.

demonstrated the influence of the poorly conserved second and third coordination spheres of the dicopper active site as strong discriminating features. Indeed, the differences in terms of activity among variously A-ring substituted aurones for a single Ty type reached up to 100-fold. The same range of variability was observed upon measuring the activity of a given aurone against Tys from different sources.

In addition, a significant improvement was provided by the HOPNO moiety in terms of TyM1 inhibition activity (e.g., IC_{50} = 1.5 μM for **1a** versus >1000 μM for the analogous 6-hydroxyaurone **V**).[17,32] To further support the potential of this group, we defined the ionization state involved in the binding. Protonation constant values for **1a−c** have thus been determined by spectrophotometric titrations in water/DMSO (90/10, w/w, see Supporting Information). Protonation constants corresponding to the HOPNO moiety (log K_{N-OH}, range 5.4−5.8) embedded on aurones indicate that at physiological pH, HOPNO moiety in **1a−c** exists exclusively in an anionic form, thereby facilitating the binding on dicopper center (Table 1). These values are lower than that of free HOPNO (6.07),[35] and lower than the protonation constants for hydroxyl groups at position 4′ of aurones **I** (R_4 = H or OH, R_6 = OH) and **II** (R_4 = R_6 = OH), in the range 8.3−8.9[36] (corroborated by classical values found for 4′-hydroxy groups of flavonoids in the literature),[37,38] indicating that these moieties are fully protonated at physiological pH. These data reinforced the potential of HOPNO contribution vs phenolic derivatives, for interacting with the copper ions.

All these elements provided the rationale to design and produce the reported HOPNO-embedded aurones. The synthesis of aurones **1a−1c** was performed according to Scheme 2 from benzofuran-3(2*H*)-one derivatives **2a−2c** (see Supporting Information).[39] We then comparatively studied hybrid aurones and HOPNO on isolated TyH. For this study, we have used a recombinant TyH produced in insect cells that was very recently validated through the evaluation of a number of known substrates and inhibitors.[4] For this enzyme we have previously determined the Michaelis−Menten kinetic parameters for L-DOPA oxidation, obtaining a K_m value of 0.34 ± 0.03 mM and a k_{cat} value of 38.1 ± 0.7 s^{-1}.[4] The effect of aurones **1a−c** on the oxidation of L-DOPA by TyH was studied. First, we verified whether TyH inhibition was concentration dependent. The kinetic behavior of TyH during the oxidation of L-DOPA was then investigated generating substrate velocities curves in the presence of various concentrations of inhibitors. The analysis of the inhibition curves indicates a competitive mode of inhibition, consistent with a direct link to the active site. The inhibition constants were then determined by nonlinear regression and curve fitting (see Supporting Information).

Scheme 2. Synthesis of Hybrid Aurones 1[a]

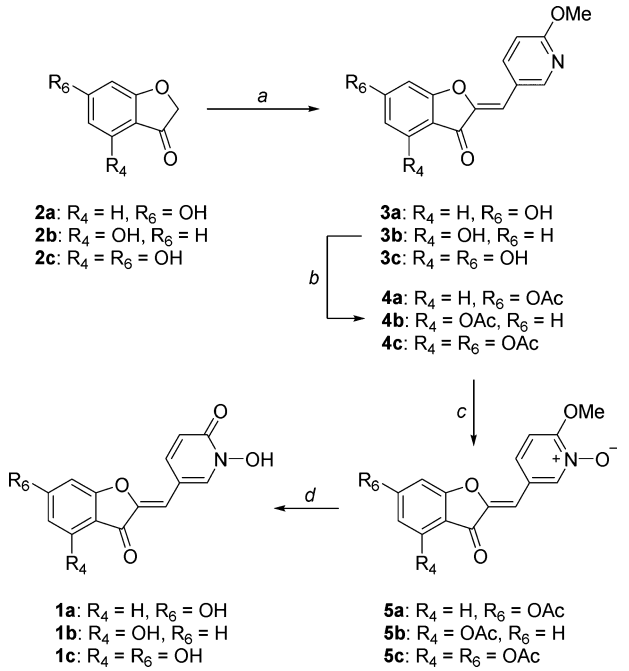

[a]Reagents and conditions: (a) 6-methoxy-3-pyridinecarboxaldehyde, KOH, MeOH, or EtOH, H_2O, 65−80 °C, 2−6 h; (b) Ac_2O, 140 °C, 5−16 h; (c) urea−H_2O_2 complex, TFAA, CH_2Cl_2, rt, 5−16 h; (d) HCl, H_2O, MeOH, 100 °C, 16−40 h.

Compounds **1b** and **1c** shared a similar inhibition potency (K_{ic} = 1.02 and 1.2 μM, respectively, Table 1), whereas analogue **1a** was found 3.5 times more active. This possibly indicates a detrimental effect of the presence of a hydroxyl group at position 4 of aurones. Interestingly, the evaluation of the HOPNO moiety in the same conditions provided very different results. Indeed, considering TyH inhibition, HOPNO was found as a very weak inhibitor, with a K_i of 128 μM, approximately 350 times higher than the value measured for compound **1a**, whereas it was previously found as a rather potent inhibitor of TyM1[34] and TyB3[40] (K_i = 1.8 and 7.7 μM, respectively). These data emphasize the crucial role of the whole aurone backbone, and not only of the embedded HOPNO moiety, in activities reported herein. Additionally, a correlation could be observed between pK_{N-OH} values and K_i values against TyH, the inhibition potency of tested compounds (including HOPNO) enhancing as deprotonation of the N−OH moiety increases.

In order to understand the reactivity of aurones with TyH and more precisely the role of the aurone backbone, theoretical studies were conducted. We focused our attention on the most

DOI: 10.1021/acsmedchemlett.6b00369
ACS Med. Chem. Lett. 2017, 8, 55−60

active hybrid aurone **1a** and comparisons were done with the interactions of the HOPNO moiety on TyH. QM/MM dynamics followed by a NCI analysis were performed. For the initial position, we made the hypothesis that **1a** and HOPNO would adopt the monodentate binding mode (Scheme 1) obtained in our previous work on TyB2[40] in which the oxygen atom of the nitrosyl group of HOPNO is fixed only on one copper atom (see Supporting Information).

The NCI method calculates an index based on the electron density and the electron density gradient.[41] This index presents singularities at low density when a weak interaction appears between two fragments. The strength of these interactions can also be calculated and isosurfaces can be plotted to visualize the domains of noncovalent interactions. Thus, the blue surfaces represent strong and attractive interactions (as hydrogen bonds), whereas the green ones indicate weak interactions (as van der Waals interactions). Figure 2 shows an average position with NCI surfaces from the TyH−HOPNO and TyH−**1a** complexes extracted from their QM/MM dynamics trajectories. If HOPNO appeared as firmly linked to one of the two copper centers in a monodentate mode, only few interactions were observed with the surrounding residues of the second coordination sphere. On the contrary, compound **1a** revealed an extended interaction pattern involving hot spot residues relatively far from the coppers, such as Ile368, Arg308, Lys306, and His304, and allowing a robust fit of **1a** inside the active site pocket. These observations are in good agreement with the aforementioned, experimentally measured K_i values.

Finally, the ability of aurones **1a−c** to suppress melanin biosynthesis in a human integrated cellular model (human melanoma MNT-1 cells) was evaluated. Results from cell lysates confirmed the potency of hybrid aurones to prevent melanogenesis in a human complex cytoplasmic environment, with an order of inhibition potency similar to that obtained from the isolated TyH inhibition assay (Table 1). Indeed, compound **1a** reached a lower IC_{50} (IC_{50} = 16.6 μM), compared to compound **1b** and compound **1c**, which obtained IC_{50} values about two times higher (IC_{50} = 30 and 34 μM, respectively). The contribution of the aurone scaffold remained very significant, as HOPNO alone had a very low activity on lysates (IC_{50} = 1300 μM). The "hybrids" revealed a limited capacity to hinder melanogenesis in MNT-1 whole cells. The recorded IC_{50} values ranged from 85.3 (for **1a**) to 120 μM (for **1b**), with a concomitant low cytotoxicity of the compounds at such concentrations, except for **1b** (Table 1). These values were thus found 3.5−5 times higher than those from lysates. These results suggest a scarce ability of hybrid compounds **1a−c** to cross MNT-1 cell membranes that may originate from the partial zwitterionic nature of the HOPNO group, as this moiety is probably experiencing a tautomeric equilibrium between the *N*-hydroxy-2-pyridinone and 2-hydroxypyridine-*N*-oxide forms. Nevertheless, HOPNO-based compounds have already demonstrated very good ability to act in cell-based and physiological contexts.[42,43] Finally it is worth noting that, at the tested conditions, the reference KA was found almost completely inactive both on lysate and whole cells.

In conclusion, a series of HOPNO-embedded aurones have been synthesized and evaluated to determine their inhibition potency against TyH and to elucidate the added value of the aurone backbone compared to the HOPNO moiety alone. If the described aurones are excellent inhibitors of TyH, a considerable gap exists in terms of inhibition potency between these compounds and the HOPNO moiety, indicating an undeniable beneficial effect of the aurone backbone, confirmed by theoretical calculation. Finally, it is worth noting that, to the best of our knowledge, compound **1a** is the most active TyH inhibitor ever reported (K_i = 0.35 μM). Its lower efficiency in suppressing melanogenesis in MNT-1 human whole cells remains to be addressed. We thus shed light on the great potential of these compounds for human-directed applications and as tools for deciphering tyrosinase role in pathologies such as melanoma.[25]

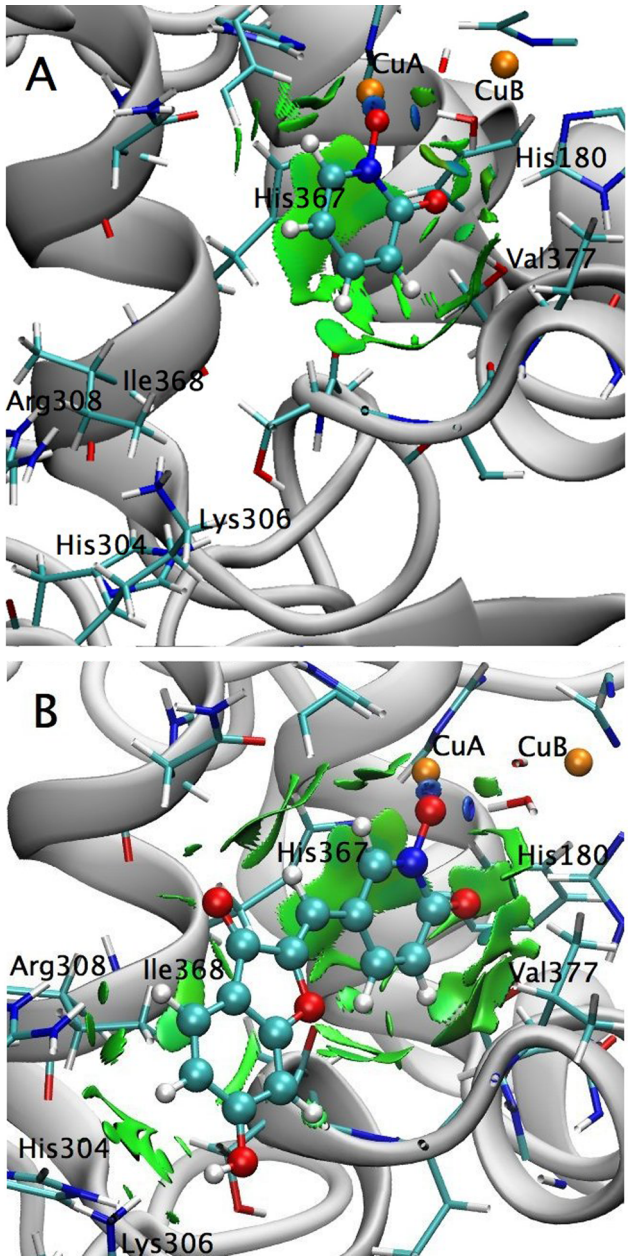

Figure 2. Average position of HOPNO−TyH (A) and **1a**−TyH (B) complexes after QM/MM dynamics. NCI surfaces (in green) represent molecular interactions and are generated with an electron density gradient value of 0.35 au (atomic units).

■ ASSOCIATED CONTENT

Supporting Information

The Supporting Information is available free of charge on the ACS Publications website at DOI: 10.1021/acsmedchemlett.6b00369.

DOI: 10.1021/acsmedchemlett.6b00369
ACS Med. Chem. Lett. 2017, 8, 55−60

Synthesis and characterizations of compounds, TyH inhibition assays, MNT-1 cellular assays, cytotoxicity assays, determination of protonation constants, computational methods, and QM/MM calculations (PDF)

AUTHOR INFORMATION

Corresponding Author

*E-mail: romain.haudecoeur@univ-grenoble-alpes.fr.

ORCID

Romain Haudecoeur: 0000-0002-6271-4717

Author Contributions

§These authors contributed equally to this work.

Notes

The authors declare no competing financial interest.

ACKNOWLEDGMENTS

The authors are grateful to ANR (Agence Nationale pour la Recherche) for financial support (Labex Arcane ANR-11-LABX-0003-01 and Blanc program 2Cu-TargMelanin ANR-09-BLAN-0028-01/02/03), ICMG (Institut de Chimie Moléculaire de Grenoble) for computer, analysis, and characterization facilities, and the European COST Program in the framework of which this work was carried out (COST action CM1003 WG 2). This work has been financed by the grant "Human recombinant tyrosinase: a testing bench for new drugs to treat melanin-related disorders" (Progetto di Ricerca di Ateneo CPDA110789/11) from the University of Padova to E.B.

ABBREVIATIONS

DOPA, 3,4-dihydroxyphenylalanine; HOPNO, 2-hydroxypyridine-*N*-oxide; KA, kojic acid; NCI, noncovalent interaction; TFAA, trifluoroacetic anhydride

REFERENCES

(1) Belle, C. In *Encyclopedia of Metalloproteins*; Kretsinger, R. H., Uversky, V. N., Permyakov, E. A., Eds.; Springer: New York, 2013; pp 574−579.

(2) Solomon, E. I.; Heppner, D. E.; Johnston, E. M.; Ginsbach, J. W.; Cirera, J.; Qayyum, M.; Kieber-Emmons, T.; Kjaergaard, C. H.; Hadt, R. G.; Tian, L. Copper active sites in biology. *Chem. Rev.* **2014**, *114*, 3659−3853.

(3) Ito, S. A chemist's view of melanogenesis. *Pigm. Cell Res.* **2003**, *16*, 230−236.

(4) Fogal, S.; Carotti, M.; Giaretta, L.; Lanciai, F.; Nogara, L.; Bubacco, L.; Bergantino, E. Human tyrosinase produced in insect cells: a landmark for the screening of new drugs addressing its activity. *Mol. Biotechnol.* **2015**, *57*, 45−57.

(5) van Gelder, C. W. G.; Flurkey, W. H.; Wichers, H. J. Sequence and structural features of plant and fungal tyrosinases. *Phytochemistry* **1997**, *45*, 1309−1323.

(6) Wang, N.; Hebert, D. N. Tyrosinase maturation through the mammalian secretory pathway: bringing color to life. *Pigm. Cell Res.* **2006**, *19*, 3−18.

(7) Sendovski, M.; Kanteev, M.; Ben-Yosef, V. S.; Adir, N.; Fishman, A. First structures of an active bacterial tyrosinase reveal copper plasticity. *J. Mol. Biol.* **2011**, *405*, 227−237.

(8) Matoba, Y.; Kumagai, T.; Yamamoto, A.; Yoshitsu, H.; Sugiyama, M. Crystallographic evidence that the dinuclear copper center of tyrosinase is flexible during catalysis. *J. Biol. Chem.* **2006**, *281*, 8981−8990.

(9) Ismaya, W. T.; Rozeboom, H. J.; Schurink, M.; Boeriu, C. G.; Wichers, H.; Dijkstra, B. W. Crystallization and preliminary X-ray crystallographic analysis of tyrosinase from the mushroom *Agaricus bisporus*. *Acta Crystallogr., Sect. F: Struct. Biol. Cryst. Commun.* **2011**, *67*, 575−578.

(10) Ismaya, W. T.; Rozeboom, H. J.; Weijn, A.; Mes, J. J.; Fusetti, F.; Wichers, H. J.; Dijkstra, B. W. Crystal structure of *Agaricus bisporus* mushroom tyrosinase: identity of the tetramer subunits and interaction with tropolone. *Biochemistry* **2011**, *50*, 5477−5486.

(11) Mauracher, S. G.; Molitor, C.; Al-Oweini, R.; Kortz, U.; Rompel, A. Crystallization and preliminary X-ray crystallographic analysis of latent isoform PPO4 mushroom (*Agaricus bisporus*) tyrosinase. *Acta Crystallogr., Sect. F: Struct. Biol. Commun.* **2014**, *70*, 263−266.

(12) Mauracher, S. G.; Molitor, C.; Al-Oweini, R.; Kortz, U.; Rompel, A. Latent and active abPPO4 mushroom tyrosinase cocrystallized with hexatungstotellurate(VI) in a single crystal. *Acta Crystallogr., Sect. D: Biol. Crystallogr.* **2014**, *70*, 2301−2315.

(13) Fujieda, N.; Yabuta, S.; Ikeda, T.; Oyama, T.; Muraki, N.; Kurisu, G.; Itoh, S. Crystal structures of copper-depleted and copper-bound fungal pro-tyrosinase: insights into endogenous cysteine-dependent copper incorporation. *J. Biol. Chem.* **2013**, *288*, 22128−22140.

(14) Bijelic, A.; Pretzler, M.; Molitor, C.; Zekiri, F.; Rompel, A. The structure of a plant tyrosinase from walnut leaves reveals the importance of "substrate-guiding residues" for enzymatic specificity. *Angew. Chem., Int. Ed.* **2015**, *54*, 14677−14680.

(15) Molitor, C.; Mauracher, S. G.; Rompel, A. Crystallization and preliminary crystallographic analysis of latent, active and recombinantly expressed aurone synthase, a polyphenol oxidase, from *Coreopsis grandiflora*. *Acta Crystallogr., Sect. F: Struct. Biol. Commun.* **2015**, *71*, 746−751.

(16) Molitor, C.; Mauracher, S. G.; Rompel, A. Aurone synthase is a catechol oxidase with hydroxylase activity and provides insights into the mechanism of plant polyphenol oxidases. *Proc. Natl. Acad. Sci. U. S. A.* **2016**, *113*, E1806−E1815.

(17) Haudecoeur, R.; Gouron, A.; Dubois, C.; Jamet, H.; Lightbody, M.; Hardré, R.; Milet, A.; Bergantino, E.; Bubacco, L.; Belle, C.; Réglier, M.; Boumendjel, A. Investigation of the binding-site homology of mushroom and bacterial tyrosinases by aurones as effectors. *ChemBioChem* **2014**, *15*, 1325−1333.

(18) Lai, X.; Soler-Lopez, M.; Wichers, H. J.; Dijkstra, B. W. Large-scale recombinant expression and purification of human tyrosinase suitable for structural studies. *PLoS One* **2016**, *11*, e0161697.

(19) Favre, E.; Daina, A.; Carrupt, P.-A.; Nurisso, A. Modeling the met form of human tyrosinase: a refined and hydrated pocket for antagonist design. *Chem. Biol. Drug Des.* **2014**, *84*, 206−215.

(20) Yaar, M. Cutaneous pigmentation in health and disease: novel and well-established players. *J. Invest. Dermatol.* **2013**, *133*, 11−13.

(21) Sehgal, V. N.; Srivastava, G. Hereditary hypo/de-pigmented dermatoses: an overview. *Int. J. Dermatol.* **2008**, *47*, 1041−1050.

(22) Brozyna, A. A.; Jozwicki, W.; Carlson, J. A.; Slominski, A. T. Melanogenesis affects overall and disease-free survival in patients with stage III and IV melanoma. *Hum. Pathol.* **2013**, *44*, 2071−2074.

(23) Chen, W.-C.; Tseng, T.-S.; Hsiao, N.-W.; Lin, Y.-L.; Wen, Z.-H.; Tsai, C.-C.; Lee, Y.-C.; Lin, H.-H.; Tsai, K.-C. Discovery of highly potent tyrosinase inhibitor, T1, with significant anti-melanogenesis ability by zebrafish in vivo assay and computational molecular modeling. *Sci. Rep.* **2015**, *5*, 7995.

(24) Gillbro, J. M.; Olsson, M. J. The melanogenesis and mechanisms of skin-lightening agents − existing and new approaches. *Int. J. Cosmet. Sci.* **2011**, *33*, 210−221.

(25) Buitrago, E.; Hardré, R.; Haudecoeur, R.; Jamet, H.; Belle, C.; Boumendjel, A.; Bubacco, L.; Réglier, M. Human tyrosinase and related proteins, are they targets for melanoma therapy? *Curr. Top. Med. Chem.* **2016**, *16*, 3033−3047.

(26) Mendes, E.; de Jesus Perry, M.; Francisco, A. P. Design and discovery of mushroom tyrosinase inhibitors and their therapeutic applications. *Expert Opin. Drug Discovery* **2014**, *9*, 533−554.

(27) Fisk, W. A.; Agbai, O.; Lev-Tov, H. A.; Sivamani, R. K. The use of botanically derived agents for hyperpigmentation: a systematic review. *J. Am. Acad. Dermatol.* **2014**, *70*, 352−365.

DOI: 10.1021/acsmedchemlett.6b00369
ACS Med. Chem. Lett. 2017, 8, 55−60

(28) Kolbe, L.; Mann, T.; Gerwat, W.; Batzer, J.; Ahlheit, S.; Scherner, C.; Wenck, H.; Stäb, F. 4-*n*-Butylresorcinol, a highly effective tyrosinase inhibitor for the topical treatment of hyperpigmentation. *J. Eur. Acad. Dermatol. Venereol.* **2013**, *27*, 19−23.
(29) Boumendjel, A. Aurones: a subclass of flavones with promising biological potential. *Curr. Med. Chem.* **2003**, *10*, 2621−2630.
(30) Haudecoeur, R.; Boumendjel, A. Recent advances in the medicinal chemistry of aurones. *Curr. Med. Chem.* **2012**, *19*, 2861−2875.
(31) Okombi, S.; Rival, D.; Bonnet, S.; Mariotte, A.-M.; Perrier, E.; Boumendjel, A. Discovery of benzylidenebenzofuran-3(2*H*)-one (aurones) as inhibitors of tyrosinase derived from human melanocytes. *J. Med. Chem.* **2006**, *49*, 329−333.
(32) Dubois, C.; Haudecoeur, R.; Orio, M.; Belle, C.; Bochot, C.; Boumendjel, A.; Hardré, R.; Jamet, H.; Réglier, M. Versatile effects of aurone structure on mushroom tyrosinase activity. *ChemBioChem* **2012**, *13*, 559−565.
(33) Markova, E.; Kotik, M.; Krenkova, A.; Man, P.; Haudecoeur, R.; Boumendjel, A.; Hardré, R.; Mekmouche, Y.; Courvoisier-Dezord, E.; Réglier, M.; Martinkova, L. Recombinant tyrosinase from *Polyporus arcularius*: overproduction in *Escherichia coli*, characterization, and use in a study of aurones as tyrosinase effectors. *J. Agric. Food Chem.* **2016**, *64*, 2925−2931.
(34) Peyroux, E.; Ghattas, W.; Hardré, R.; Giorgi, M.; Faure, B.; Simaan, A. J.; Belle, C.; Réglier, M. Binding of 2-hydroxypyridine-*N*-oxide on dicopper(II) centers: insights into tyrosinase inhibition mechanism by transition-state analogs. *Inorg. Chem.* **2009**, *48*, 10874−10876.
(35) Orio, M.; Bochot, C.; Dubois, C.; Gellon, G.; Hardré, R.; Jamet, H.; Luneau, D.; Philouze, C.; Réglier, M.; Serratrice, G.; Belle, C. The versatile binding mode of transition-state analogue inhibitors of tyrosinase towards dicopper(II) model complexes: experimental and theoretical investigations. *Chem. - Eur. J.* **2011**, *17*, 13482−13494.
(36) Haudecoeur, R. MSc Thesis, Univ. Joseph-Fourier, Grenoble, 2008.
(37) Herrero-Martinez, J. M.; Sanmartin, M.; Roses, M.; Bosch, E.; Rafols, C. Determination of dissociation constants of flavonoids by capillary electrophoresis. *Electrophoresis* **2005**, *26*, 1886−1895.
(38) Musialik, M.; Kuzmicz, R.; Pawlowski, T. S.; Litwinienko, G. Acidity of hydroxyl groups: an overlooked influence on antiradical properties of flavonoids. *J. Org. Chem.* **2009**, *74*, 2699−2709.
(39) Haudecoeur, R.; Ahmed-Belkacem, A.; Yi, W.; Fortuné, A.; Brillet, R.; Belle, C.; Nicolle, E.; Pallier, C.; Pawlotsky, J.-M.; Boumendjel, A. Discovery of naturally occurring aurones that are potent allosteric inhibitors of hepatitis C virus RNA-dependent RNA polymerase. *J. Med. Chem.* **2011**, *54*, 5395−5402.
(40) Bochot, C.; Favre, E.; Dubois, C.; Baptiste, B.; Bubacco, L.; Carrupt, P.-A.; Gellon, G.; Hardré, R.; Luneau, D.; Moreau, Y.; Nurisso, A.; Réglier, M.; Serratrice, G.; Belle, C.; Jamet, H. Unsymmetrical binding modes of the HOPNO inhibitor of tyrosinase: from model complexes to the enzyme. *Chem. - Eur. J.* **2013**, *19*, 3655−3664.
(41) Johnson, E. R.; Keinan, S.; Mori-Sanchez, P.; Contreras-Garcia, J.; Cohen, A. J.; Yang, W. Revealing noncovalent interactions. *J. Am. Chem. Soc.* **2010**, *132*, 6498−6506.
(42) Liu, Z.; Yao, Y.; Kogiso, M.; Zheng, B.; Deng, L.; Qiu, J. J.; Dong, S.; Lv, H.; Gallo, J. M.; Li, X.-N.; Song, Y. Inhibition of cancer-associated mutant isocitrate dehydrogenases: synthesis, structure−activity relationship, and selective antitumor activity. *J. Med. Chem.* **2014**, *57*, 8307−8318.
(43) Subissi, A.; Monti, D.; Togni, G.; Mailland, F. Ciclopirox. Recent nonclinical and clinical data relevant to its use as a topical antimycotic agent. *Drugs* **2010**, *70*, 2133−2152.

DOI: 10.1021/acsmedchemlett.6b00369
ACS Med. Chem. Lett. 2017, 8, 55−60